Bulgarian Journal of Physics vol. **XX** (20XX) 1–11

Effect of Pseudo-Hybridization Interaction on Ground State and Finite Temperature Properties of Mixed Valence Systems

Piyali Ghosh, **Nanda Kumar Ghosh***
Department of Physics, University of Kalyani,
Kalyani-741235, West Bengal, India
*Corresponding author Email: nkg@klyuniv.ac.in

Received *28 May 2024*

Abstract. Pseudo-hybridization interaction (g) acting between f- and d-electrons situated on same site induced by d-electron density with opposite spin, has been considered within a two-band extended Falicov-Kimball model. An exact diagonalization method in an eight-site 2D square cluster has been followed. The obtained results are: (i) a discontinuous intermediate valence transition at a critical value of f-level energy E_c; (ii) non-zero f–d correlation function which confirms the valence transition from insulating state to metallic state; (iii) single- and double-peak shaped temperature dependent specific heat curves in the presence of pseudo-hybridization interaction and for different f-level energy E; (iv) increasing order of the system with the increase of g; (v) sharp peak of temperature dependent spin susceptibility curves confirm the antiferromagnetic property of the system. The results have been compared with earlier observations.

KEY WORDS: Mixed valence compound, Extended Falicov-Kimball model, Pseudo-hybridization interaction, Exact diagonalization method, Valence transition, Antiferromagnetic property.

1 Introduction

Due to the fluctuating electronic configuration of some rare earth elements, their compounds (like SmS, SmB_6, SmSe, SmTe, etc.) show unusual variety of thermodynamical, electrical and magnetic properties [1]. The usual electronic configuration of such rare earth compounds is $(4f)^n(sd)^m$. By the application of pressure (as well as temperature) which increases the f-level energy E, the $4f$ shell loses its stability. These rare earth compounds are referred to as mixed valence (MV) compounds because two valence states $(4f)^n(sd)^m$ and $(4f)^{n-1}(sd)^{m+1}$ coexist with one another. They exist with the variable oxidation number in their compounds. The f-level electrons become partially band like nature and the average number of f-electrons per site, i.e., valence turns into non-integral in value. Thus, the non-integral valence makes the properties

of mixed-valent compounds anomalous [2]. Due to the anomalous properties, they have diverse applications in the modern civilization. Components of many computer parts such as DVD, hard-disk, CD-ROM are made with rare earth magnets. In petroleum refining process, lanthanum-based catalysts are used. One of the most surprising applications of rare earth compounds has been implemented in the field of cancer treatment specially in cancer diagnosis and therapy [3].

In a homogeneous mixed-valence compound, i.e., SmB_6, the ratio of two ions Sm^{2+} and Sm^{3+} is 4:6. Many experiments on SmB_6 establish that the ionic configuration of samarium is an admixture of $4f^6$ and $4f^5$ added with a $5d$ characterized and localized electron [4–6]. At normal pressure, the rare earth element lanthanum (or its compound) exhibits the superconducting nature due to the particular position of the $4f$ states. Its critical temperature vary from 5.2 K at atmospheric pressure to 9.3 K at 40 kbar. The rare-earth element Cerium also exhibits superconducting nature at pressures higher than 50 kbar with a T_c equal to 1.5 K [7]. Some rare earth compounds, i.e., LuB_{12}, LaB_6, $CeCu_2Si_2$, $CeRu_3Si_2$ etc. exhibit superconducting as well as mixed valence property [8, 9].

The various anomalous properties of MV compounds were studied experimentally as well as theoretically. Many models and methods have been used to describe the effects of various interactions on the properties of MV compounds. L_{III} absorption edge spectrum of x-ray of samarium hexaboride (SmB_6) proves the existence of two peaks due to Sm^{2+} and Sm^{3+} ions [4]. Several performed experiments help to understand the anomalous properties of MV systems [10]. Measurements on temperature dependence of resistance [11], low temperature specific heat [12], magnetoresistance [13], electronic specific heat coefficient [14] etc. confirm the anomalous character of MV compound.

In [15], using Monte Carlo method, the Ising model is extended with the first, second, third and fourth nearest-neighbor spin couplings to study the magnetic properties of rare-earth tetraborides. In [16], the DFT (density functional theory) is applied to investigate the electronic properties of rare earth compound SmB_6. Moreover, on rare earth tetraborides a numerical study is made using the combined model of Falicov-Kimball and Ising type [17]. Studies on Falicov-Kimball model using various methods are still being continued through ongoing research works. In the one-dimensional spin-1/2 Falicov-Kimball model, the density-matrix-renormalization-group approach is utilized to investigate the impact of external magnetic field on the stability of the excitonic phase caused by local hybridization [18]. The ground state features of the spinless Falicov-Kimball model extended by f-electron hopping and nonlocal hybridization with inversion symmetry are investigated in two and three dimensions using the Hartree-Fock (HF) approximation with charge- density- wave (CDW) instability [19]. The spin-one-half Falicov-Kimball model with the Ising-type Hund coupling is studied using the density matrix renormalization group (DMRG) approach to examine the effects of several parameters on the stability of charge and spin order [20]. By using the exact diagonalization as well as Quantum Monte Carlo

study, magnetization process in case of rare-earth tetraborides are described for the spin-electron model [21].

The conventional Falicov-Kimball model [22] is extended by various type of interactions, occurred in mixed valence compounds. For instance, correlated hopping [23], electron-phonon interaction [24–26], nonlocal Coulomb interaction [27], next-nearest-neighbor (NNN) hopping interaction [28], NNN Coulomb interaction [29], next-to-next-nearest-neighbor hopping interaction [30] etc. are already studied. Temperature dependence of heat capacity of mixed-valent $CeNi_4Cr$ compound have been experimentally measured [31]. In [32], few interactions like Coulomb interaction, Hubbard type interaction, pseudo-hybridization interaction are studied only on the rare earth element Lanthanum. Hubbard type interaction [33], Coulomb interaction [29] are studied in mixed valence system. But the pseudo-hybridization is not studied well, still now, for any rare earth compounds. The interaction of central importance for this work is the pseudo-hybridization which acts when two electrons are on the same site. This hybridization term constitutes the channel which allows one of these d-electrons to occupy a f-site.

In the present communication, we have considered a 2D square lattice with 8-sites to explain the effect of pseudo-hybridization on the valence transition of rare-earth mixed-valent compounds. Thermodynamic properties like specific heat, entropy and susceptibility have also been studied. We have followed Lanczos exact diagonalization method to avoid any error due to approximations taken. However, finite size effects cannot be ignored in a finite size cluster embedded in a self-consistent host representing the rest of the system. Here, the interaction considered is up to nearest-neighbour (NN) sites only. Moreover, we have not performed any calculation considering long-range correlations in which finite size effect is dominant. Therefore, the results obtained here can establish the behaviour of rare-earth MV compounds, at least qualitatively.

2 Hamiltonian and Formulation

The cluster of a 2D square lattice with two bands and eight sites, is taken into consideration here. The considered Hamiltonian of our present study is

$$H = H_0 + H' \,, \tag{1}$$

where

$$\begin{aligned} H_0 = {} & E \sum_{i\sigma} f^+_{i\sigma} f_{i\sigma} + U \sum_i f^+_{i\uparrow} f_{i\uparrow} f^+_{i\downarrow} f_{i\downarrow} + G \sum_{i\sigma\sigma'} f^+_{i\sigma} f_{i\sigma} d^+_{i\sigma'} d_{i\sigma'} \\ & + V \sum_{\langle i,j\rangle\sigma} (f^+_{i\sigma} d_{j\sigma} + d^+_{j\sigma} f_{i\sigma}) - t \sum_{\langle i,j\rangle\sigma} d^+_{i\sigma} d_{j\sigma} \,; \end{aligned} \tag{2}$$

$$H' = g \sum_{i\sigma} [f^+_{i\sigma} d_{i\sigma} + d^+_{i\sigma} f_{i\sigma}] d^+_{i,-\sigma} d_{i,-\sigma} \,, \tag{3}$$

where i and j sites are all pairs of nearest neighbours on the 2D square lattice; the creation and annihilation operators are denoted by $f^+_{i\sigma}$ and $f_{i\sigma}$ for localized f-electrons and $d^+_{i\sigma}$, $d_{i\sigma}$ for itinerant d-electrons respectively; spin of electron is denoted by σ, σ'. E is the energy at the f-level; U denotes the on-site Coulomb interaction; G stands for the Coulomb type interaction acting between f- and d-electrons; V represents the hybridization interaction acting between f- and d-electrons; t is d-electron quantum mechanical hopping between nearest neighbour sites. H' is the pseudo-hybridisation interaction where g is the strength of the interaction.

The considered basis states, calculated on eight-site is in the following form:

$$|n^f_{1\uparrow}n^f_{1\downarrow}n^d_{1\uparrow}n^d_{1\downarrow}n^f_{2\uparrow}n^f_{2\downarrow}n^d_{2\uparrow}n^d_{2\downarrow}n^f_{3\uparrow}n^f_{3\downarrow}n^d_{3\uparrow}n^d_{3\downarrow}.....n^f_{8\uparrow}n^f_{8\downarrow}n^d_{8\uparrow}n^d_{8\downarrow}\rangle\,. \quad (4)$$

The eigenvectors of H are produced by the linear combination of the basis vectors as in eq. (4):

- f-electron density: $\langle n^f_i\rangle = \dfrac{1}{N}\sum_{i\sigma} f^+_{i\sigma}f_{i\sigma}$,
  where N stands for the number of lattice sites;
- The function of inter-site f-d correlation: $C_{fd} = \langle f^+_{i\sigma}d_{j\sigma}\rangle$;
- For each lattice site, entropy is $S = \dfrac{1}{N}(k_B lnZ + \dfrac{\langle H\rangle}{T})$;
- Low-temperature specific heat is $C = k_B\beta^2\dfrac{\partial^2}{\partial\beta^2}\ln Z$,
  where $Z = \sum_a e^{-\beta E_a}$, the total partition function is calculated over all basis states, the corresponding eigenvalues are E'_as and $\beta = \dfrac{1}{k_B T}$,
  k_B is the Boltzmann constant. k_B is taken to be one throughout our present study;
- f-electron spin susceptibility is denoted by $\chi = \beta\langle(n^f_{i\uparrow} - n^f_{i\downarrow})^2\rangle$;
- $\dfrac{1}{\chi}$ represents the reciprocal susceptibility.

3 Results and Discussions

The number of electrons taken in this communication is limited to 2. The results of several experimental observations provide the values of parameters used in this paper. The strength of the nearest-neighbor hopping between d-electrons is taken as unity. The strengths of other interactions are taken comparatively. The unit of the strengths are arbitrary [30].

First observation in Figure 1 is that the value of f-electron density $\langle n^f_i\rangle$ decreases from a maximum value near equals to 0.17 (approximately) with the increasing value of f-level energy (E) which is characterised by imposed external pressure or temperature. Then it becomes almost saturation near the zero

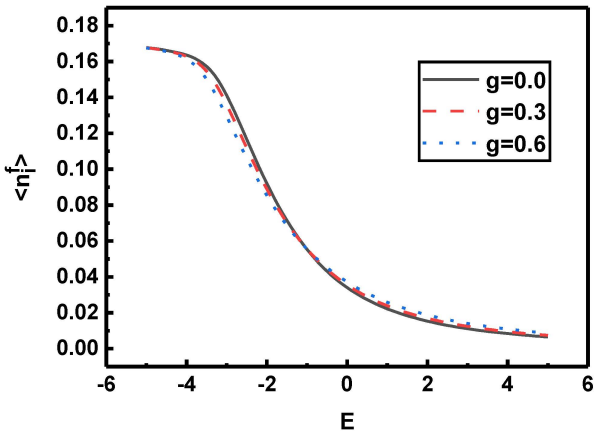

Figure 1. Variation of f-electron density $\langle n_i^f \rangle$ with E for distinct values of pseudo hybridisation interaction g. Here $U = 5.0$, $G = 1.0$, $V = 0.5$, $t = 1.0$.

value of $\langle n_i^f \rangle$ in spite of the increasing value of E. So, it can be said that a transition from insulator to metallic state of MV system is occurred due to the pseudo hybridisation interaction. According to a comparison of our findings with earlier research, similar valence transitions have been seen in ref. [34, 35]. This first order valence transition is happened at a particular value of $E = E_c$ (approximately). E_c is different for different curves. We observe that valence transition is less sharp for higher value of g. The splitting of the graphs ensures about the effect of pseudo-hybridisation interaction on MV compounds.

Non zero value of f-d correlation function (C_{fd}) implies that an intermediate valence transition from insulating to metallic condition is occurred in MV system. If the value of C_{fd} is zero then the system will be either in insulating state or metallic state [36]. From Figure 2, it is observed that C_{fd} decreases with the increasing value of E up to a critical value of E, i.e. E_c. After the attainment of E_c, it further shows increasing property with the increase of E. E_c is very close for different graphs of different values of g. In the region $E < E_c$, the system is more insulating for lower value of g and in region $E > E_c$, the system is more metallic in case of lower value of g. The splitting of the graphs for various values of g proves the existence of the pseudo-hybridization interaction in MV systems.

Figure 3 reveals the nature of curves, plotted between entropy (S) and temperature. As T tends to zero, entropy goes to zero and system becomes disordered as T increases. In Figure 3, we observe that the system becomes more ordered state with the increasing value of pseudo-hybridisation interaction. At the low temperature region $0.25 < T < 0.75$ (approximately), the splitting of the graphs is clearly visible which emphasizes on the existence of the effect due to pseudo

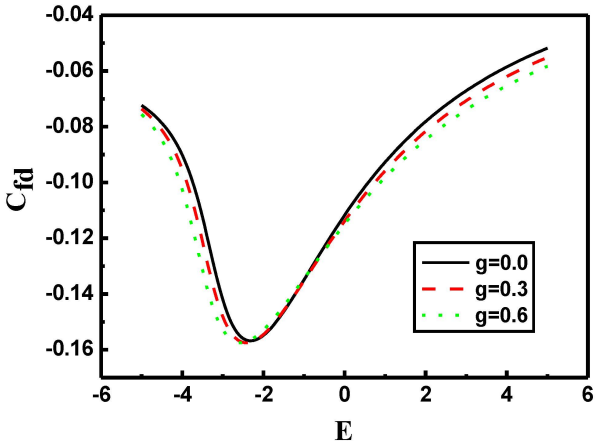

Figure 2. f–d corelation function vs. E curves for distinct values of g. Here $U = 5.0$, $G = 1.0$, $V = 0.5$, $t = 1.0$.

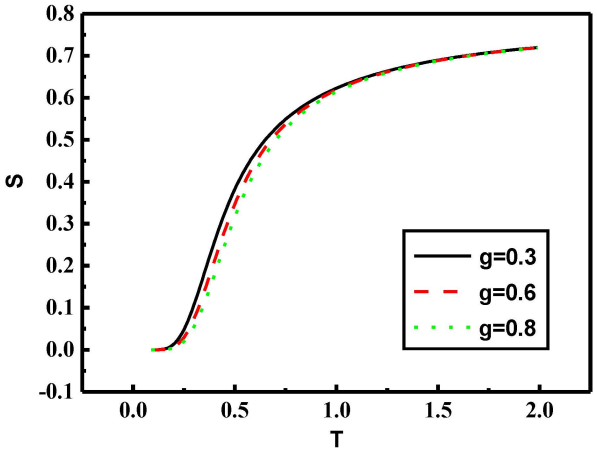

Figure 3. Temperature dependent variation of entropy for different g values. Here $E = -2.0$, $U = 5.0$, $G = 1.0$, $V = 0.5$, $t = 1.0$.

hybridisation interaction. Further, this temperature region can be identified as the transition temperature T_c region [37]. For higher temperatures, i.e., $T > 1.5$ (approximately) all graphs, plotted for distinct values of g are converged in perfectly and system becomes completely disordered state.

To investigate the variation of specific heat with temperature, we have plotted the temperature-dependent specific heat graphs in Figure 4 and Figure 5 varying with g and E respectively. In Figure 4, initially specific heat increases with the increasing value of temperature up to a certain value of temperature which

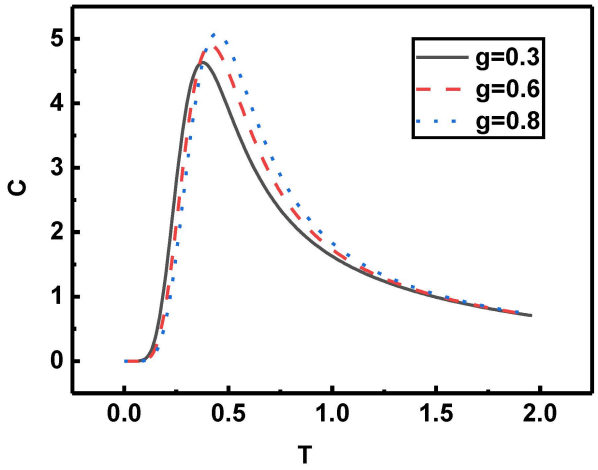

Figure 4. Variation of Specific heat (C) with temperature for distinct values of g. Here $E = -2.0$, $U = 5.0$, $G = 1.0$, $V = 0.5$, $t = 1.0$.

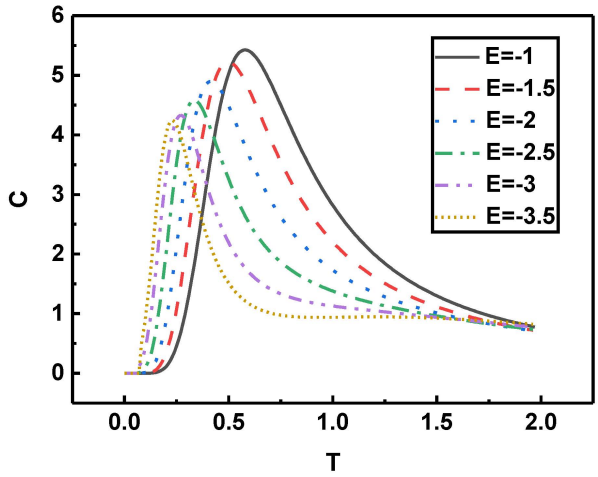

Figure 5. Temperature dependent variation of specific heat (C) for distinct values of f-level energy (E). Here $U = 5.0$, $G = 1.0$, $V = 0.5$, $t = 1.0$, $g = 0.6$.

shifts to higher region of temperature with the increasing value of g. After the attainment of the peak, specific heat decreases with the increase of T. The peak, shown in the curve implies the valence transition, occurred in mixed valence system due to pseudo-hybridisation interaction. It is also noticeable that the peak height increases with the increasing value of g. At higher values of T, i.e., $T > 1.1$ (approximately) all graphs are merged to get a saturation condition. In Figure 4, the specific heat curves at low temperatures show the single peak

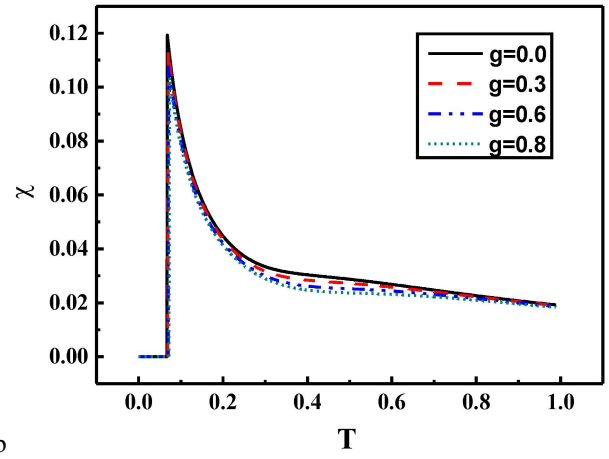

htb

Figure 6. Spin susceptibility as a function of temperature for different values of g. Here $E = -2.0, U = 5.0, G = 1.0, V = 0.5, t = 1.0$.

structure for higher values of critical f- level energy E [10]. These results are in good agreement with the experimental observations [31].

The observations of Figure 5 are that for $-1 > E \leq -2$ (approximately), the graphs show only single peak but for $E < -2$ the curves show double peak [12]. The height of the first sharp peak increases and also shifts to the higher temperature region with the increasing value of E. The sharp shaped peak is due to the presence of large number of many-body states which are very close to the ground state. The wide peak with comparatively short in height is generated due to Schottky-effect [38]. With the decrease of E, the second broad peak becomes more prominent in nature.

For various values of g , Figure 6 illustrates the changes of spin susceptibility with temperature. The observations of Figure 6 are: (a) the graphs show very sharp peak at lower temperature region. MV compound TmSe shows similar Curie contribution and is ordered antiferromagnetically [1]; (b) Neel temperature (T_N) where the spin susceptibility is at its highest, is almost in same value for each graph; and (c) the peak height increases with the decreasing value of g. The peak of susceptibility curves ensures about the antiferromagnetic property of the material [39, 40]. Furthermore, we observe that there is a good coincidence of all susceptibility curves towards zero-spin susceptibility in the region $T < T_N$.

4 Conclusion

In summary, exact diagonalization study on the properties like valence transition, thermodynamic and magnetic properties of MV compounds have been carried out. A discontinuous curve of f-electron density versus E confirms the valence transition from insulator to metal. The study of f-d correlation function C_{fd} with E shows that with increasing E, initially C_{fd} decreases and after a certain minimum value it again increases. The non-zero value of this function also confirms that the system goes through a valence transition from insulator to metal due to pseudo-hybridisation interaction. Though there is a finite size limitation in our present study but the obtained results can help to study for large lattice cluster without changing the basic conclusion [41]. Disorder in the system is in inversely proportional with pseudo hybridisation interaction. Our considered system becomes more ordered state with the increasing value of g. In the low temperature variation of specific heat curves, a single peak at low temperature region is observed which is due to Schottky-effect. Single peak as well as double peak nature of specific heat curves have been observed for this system for different values of g and E. Many body states are responsible for the sharp peak of specific heat curve of the system. The temperature variation of spin susceptibility curve reveals the antiferromagnetic behaviour of mixed valence system. We hope our theoretical observations should support to the future implementation in modern life and technology.

Funding declaration

The work has been financially supported under RUSA 10 component (CH and E) No. IP/RUSA (C-10)/05/2021 of the University of Kalyani.

Acknowledgement

We are grateful to the University of Kalyani for the infrastructural support.

References

[1] C.M. Varma (1976) Mixed-valence compounds. *Rev. Mod. Phys*. **48** 219-238.

[2] J.M. Robinson (1979) Valence transitions and intermediate valence states in rare earth and actinide materials. *Phys. Rep.* **51** 1-62.

[3] J. Wang, S. Li (2022) Applications of rare earth elements in cancer: Evidence mapping and scientometric analysis. *Front. Med.* **9** 2282-2294.

[4] M. Mizumaki, S. Tsutsui, F. Iga (2009) Temperature dependence of Sm valence in SmB_6 studied by X-ray absorption spectroscopy. *J. Phys.: Conf. Ser.* **176** 012034-012038.

[5] J.N. Chazalviel, M. Campagna, G.K. Wertheim, P.H. Schmidt (1976) Configurational mixing and $4f$-photoemission lineshapes in SmB_6. *Solid State Commun.* **19** 725-728.

[6] R.L. Cohen, M. Eibschütz, K.W. West (1970) Electronic and Magnetic Structure of SmB_6. *Phys. Rev. Lett.* **24** 383-386.

[7] C.F. Ratto, B. Coqblin, E.G. d'Agliano (1969) Superconductivity of lanthanum and cerium at high pressures. *Adv. Phys.* **18** 489-513.

[8] S. Gabani, K. Flachbart, K. Siemensmeyer, T. Mori (2020) Magnetism and superconductivity of rare earth borides. *J. Alloys Compd.* **821** 153201-153250.

[9] D. Johrendt (2020) Rare earth based superconducting materials. In: *Rare Earth Chemistry*, eds. R. Pöttgen, T. Jüstel, C.A. Strassert. De Gruyter STEM, pp. 557-575.

[10] J.M. Lawrence, P.S. Riseborough, R.D. Parks (1981) Valence fluctuation phenomena. *Rep. Prog. Phys.* **44** 1-85.

[11] A. Menth, E. Buehler, T.H. Geballe (1969) Magnetic and semiconducting properties of SmB_6. *Phys. Rev. Lett.* **22** 295-297.

[12] L.J. Sundström (1978) Low temperature heat capacity of the rare earth metals. *Handbook on the physics and chemistry of rare earths* **1** 379-410.

[13] H. Hartmann, K. Berggold, S. Jodlauk, I. Klassen, K. Kordonis, T. Fickenscher, T. Lorenz (2005) Magnetoresistance, specific heat and magnetocaloric effect of equiatomic rare-earth transition-metal magnesium compounds. *J. Phys.: Condens. Matter* **17** 7731-7742.

[14] K. Sato, Y. Isikawa, K. Mori (1992) Magnetic specific heat of light rare earth Heusler compounds $RInCu_2$, (R = La, Ce, Pr, Nd and Sm). *J. Magn. Magn. Mater.* **104** 1435-1436.

[15] H. Čenčariková, P. Farkašovský (2015) Fractional magnetization plateaus in the extended Ising model on the Shastry–Sutherland lattice: Application to rare-earth metal tetraborides. *phys. stat. sol (b)* **252** 333-338.

[16] M. Gmitra, H. Čenčariková, P. Farkašovský (2014) First-Principles Study of Kondo Insulator SmB_6. *Acta. Phys. Pol. A* **126** 298-299.

[17] P. Farkašovský, H. Čenčariková, S. Mataš (2010) Numerical study of magnetization processes in rare-earth tetraborides. *Phys. Rev. B* **82** 054409-054415.

[18] P. Farkašovský (2024) Influence of magnetic field on the electronic ferroelectricity in the external Falicov-Kimball model. *J. Phys: Condens. Matter* **36** 085601-085606.

[19] P. Farkašovský (2023) Hartree-Fock exploration of electronic ferroelectricity, valence transitions, and metal-insulator transitions in the extended Falicov-Kimball model. *Phys. Rev. B.* **108** 075161.

[20] P. Farkašovský (2023) On the stability of charge and spin order in the spin-one-half Falicov-Kimball model with the Ising-type Hund coupling. *J. Magn. Magn. Mater.* **573** 170659.

[21] P. Farkašovský, L. Regeciová (2020) Formation of Magnetization Plateaus in Rare Earth Tetraborides: Exact Diagonalization and Quantum Monte Carlo Studies. *J. Supercond. Nov. Magn.* **33** 3463-3467.

[22] L.M. Falicov, J.C. Kimball (1969) Simple model for semiconductor-metal transitions: SmB_6 and transition-metal oxides. *Phys. Rev. Lett.* **22** 997-999.

[23] N.K. Ghosh, S.K. Bhowmick, N.S. Mondal (2011) Role of correlated hopping in mixed valence phenomena. *Pramana - J. Phys.* **76** 139-147.

[24] N.K. Ghosh, S.C. Ghosh, R.L. Sarkar (1990) Electron–Phonon Interaction Induced Hybridisation in Mixed-Valence Systems. *phys. stat. sol (b)* **158** 223-228.

[25] S.C. Ghosh, N.K. Ghosh, R.L. Sarkar (1990) Role of Electron-Phonon Interaction Induced Hybridisation in Spin Included Mixed-Valence Phenomena. *phys. stat. sol. (b)* **161** 661-666.

[26] S.K. Bhowmick, N.K. Ghosh (2011) Falicov-Kimball model extended by electron-phonon interaction (EPI). *Armen. J. Phys.* **4** 30-37.

[27] P. Farkašovský (2019) The influence of nonlocal interactions on valence transitions and formation of excitonic bound states in the generalized Falicov–Kimball model. *Eur. Phys. J. B* **92** 1-5.

[28] S.K. Bhowmick, N.K. Ghosh (2012) Falicov-Kimball model extended by next–nearest–neighbor (NNN) hopping of d-electrons. *Indian J. Phys.* **86** 345-349.

[29] P. Mukherjee, N.K. Ghosh (2018) Impact of NNN Coulomb Interaction on the Properties of Mixed Valence Compounds. *Int. J. Curr. Trends Sci. Technol*. **8** 20195-20202.

[30] P. Ghosh, N.K. Ghosh (2022) Effect of next to next-nearest-neighbor (NNNN) hopping interaction in mixed valence systems and study of the thermodynamic properties. *IOP Conference Series: Materials Science and Engineering* **1258** 012005-012010. IOP Publishing.

[31] M. Zapotokova, M. Reiffers (2022) $CeNi_4Cr$ compounds and its thermodynamic properties. *J. Phys.: Conf. Ser*. **2164** 012055-012059.

[32] F. Weling (1978) A two-band Hubbard-model description of an almost mixed valence system: A new ground state for La. *J. Phys. C: Solid State Phys*. **11** 3225-3234.

[33] P. Mukherjee, N.K. Ghosh (2017) Signatures of hubbard type interaction in mixed-valent systems. *Bull. Pure Appl. Sci*. **36D** 124-130.

[34] H. Čenčariková, P. Farkašovský, M. Žonda (2008) The influence of nonlocal coulomb interaction on ground-state properties of the Falicov–Kimball model in one and two dimensions. *Int. J. Mod. Phys. B* **22** 2473-2487.

[35] P. Farkašovský (1997) Some exact results for the spin-1/2 Falicov-Kimball model in the strong coupling limit. *Z. Phys. B* **104** 147-151.

[36] P. Entel, H.J. Leder, N. Grewe (1978) Phonon induced instabilities in intermediate valence compounds. *Z. Phys. B* **30** 277-285.

[37] N.S. Mondal, N.K. Ghosh (2010) Role of next-nearest-neighbour hopping in the internal structure of the ground state and finite temperature quantities of 2D $t-J$ model. *Pramana – J. Phys.* **74** 1009-1015.

[38] S.D. Bader, N.E. Phillips, D.B. McWhan (1973) Heat capacity and resistivity of metallic SmS at high Pressure. *Phys. Rev. B* **7** 4686-4688.

[39] C. Kittel (2007) *Introduction to Solid State Physics*, 7th ed. Wiley India Pvt. Ltd.

[40] P. Farkašovský, L. Regeciová (2022) Ground state and thermodynamic properties of the coupled double-Ising model: application to rare-earth tetraborides. *J. Phys.: Condens. Matter* **34** 435802-435827.

[41] K. Roy, S. Ghosh, S. Nath, N.K. Ghosh (2019) Specific heat, entropy and magnetic properties of high T_c superconductivity within the planar $t-t'-J-V$ model. *Eur. Phys. J. B* **92** 1-10.